Segmentation of MRI Using Hierarchical Markov Random Field*

ZHANG Hong-mei[1], YUAN Ze-jian[2], CAI Zhong-min[3], BIAN Zheng-zhong[1]

[1](*School of Life Science and Technology*, *Xi'an Jiaotong University*, *Xi'an* 710049, *China*);

[2](*Institute of Artificial Intelligence and Robotics*, *Xi'an Jiaotong University*, *Xi'an* 710049, *China*);

[3](*Institute of System Engineering*, *Xi'an Jiaotong University*, *Xi'an* 710049, *China*)

E-mail: clara_mei@yeah.net

http://www.xjtu.edu.cn

Received February 1, 2002; accepted April 29, 2002

Abstract: Magnetic Resonance Image (MRI) segmentation plays a major role in the tissue quantitative analysis which benefits the early treatment of neurological diseases. In this paper, a new approach to MRI segmentation based on hierarchical Markov random field (MRF) model is proposed: In higher-level MRF, a new mixture model is presented to describe the label image, that is, the interior of region is modeled by homogenous and isotropic MRF while the boundary is modeled by inhomogeneous and anisotropic MRF. So the orientation is incorporated into the boundary information and the characteristic of label image can be more accurately represented. In lower-level MRF, the different Gauss texture is filled in each region to describe pixel image. Then the segmentation problem is formulated as Maximum a Posterior Probability (MAP) estimation rule. A histogram based DAEM algorithm is used, which is able to find the global optima of the standard finite normal mixture (SFNM) parameters. Based on the meaning of prior MRF parameter, an approximate method is proposed to simplify the estimation of those parameters. Experiments on the pathological MRI show that our approach can achieve better results.

Key words: hierarchical Markov random field; SFNM; image segmentation; MRI; MAP

Image segmentation is a very important tool in clinical application. It is employed in image guided monitoring, computer intervention. Pathological studies show that many neurological diseases are accompanied by subtle abnormal changes in brain tissues. Quantitative analysis of MRI does great help on early treatment[1~5].

In hierarchical MRF, the higher level MRF determines the prior of label image for the region formation process, while the lower level MRF contributes to the conditional probability of the pixel image in each region[6]. Here we propose a new mixture model to describe the higher-level label image. The formation of label image is composed of two components: (1) A homogenous and isotropic MRF is used to characterize the interior of region and (2) an inhomogeneous and anisotropic MRF is used to characterize the boundary. While in the lower-level MRF, each region is filled with the different Gauss texture to form the pixel image. According to Maximum a Posterior

* Supported by the National Natural Science Foundation of China under Grant No.60071029 (国家自然科学基金) and the Creative Research Group Science Foundation of China under Grant No.60024301(国家创新研究群体科学基金)

ZHANG Hong-mei was born in 1973. She is a Ph.D. candidate at the School of Life Science and Technology, Xi'an Jiaotong University. Her research interests are medical image segmentation and image fusion. **YUAN Ze-jian** was born in 1971. He is a Ph.D. candidate at the Institute of Artificial Intelligence and Robotics, Xi'an Jiaotong University. His research interests are image processing and pattern recognition. **CAI Zhong-min** was born in 1975. He is a Ph.D. candidate at the System Engineering Institute, Xi'an Jiaotong University. His research interests are network security and intrusion detection. **BIAN Zheng-zhong** was born in 1938. He is a professor and doctor supervisor at the School of Life Science and Technology, Xi'an Jiaotong University. His research interests are medical signal processing.

Probability (MAP) rule, the parameters of the two levels could be estimated respectively and iteratively. Compared with the previous researches[3,5,7,8], our work have the following contributions:

1) A new mixture MRF model is proposed to establish the label image. In contrast to the previous models[1,2,4,8], the four prior clique parameters $\{\beta_i^{(1)},\beta_i^{(2)},\beta_i^{(3)},\beta_i^{(4)}\}$ associated with pixel i are taken into account on the boundary. So orientation is considered and the characteristic of label image can be more accurately represented.

2) The estimation of SFNM parameters in Ref.[1] was based on EM algorithm, which may trap into local optima and is sensitive to the initial value. Here we derive a histogram based DAEM algorithm to find global optima.

3) Based on the actual meaning, an approximate but simple method is proposed to estimate the MRF prior parameters. Then according to Iterated Conditional Modes (ICM) algorithm, the label image is updated sequentially.

Experiments on a pathological MRI showed our approach achieves better results than previous research. The performance evaluation is done via AIC criteria and the post-global relative entropy (GRE).

The rest of the paper is organized as follows. In Section 1, the model is described. In Section 2, the parameter estimation method is discussed in detail. In Section 3, the experiment results are compared with previous work. In Section 4, the future work is discussed.

1 Image Model

1.1 Lower-Lever MRF

Let S denote a 2-dimensional integer lattice and represent points in S by $i=(r_1,r_2)\in S$. The image X is a random field defined on S. Based on hierarchical MRF, we suppose the pixel gray in the k-th region obey a normal distribution of mean μ_k and variance $\sigma^2_k(k=1,2,\ldots,K)$. Then we can represent the histogram of the image as a standard finite normal mixture (SFNM):

$$f(x)=\sum_{k=1}^{K}c_k\cdot\frac{1}{\sqrt{2\pi}\sigma_k}\exp\{-\frac{(x-\mu_k)^2}{2\sigma_k^2}\}\triangleq\sum_{k=1}^{K}c_k\cdot g(x\mid\mu_k,\sigma_k^2)\,, \tag{1}$$

where c_k is the mixture ratio of the k-th Gauss kernel and satisfies

$$\sum_{k=1}^{K}c_k=1,\quad(0\le c_k\le 1)\quad, \tag{2}$$

K is the adaptive number of the class which will be determined by AIC criteria.

1.2 Higher-Lever MRF

The label image is denoted as $l=\{l_i\mid i\in S\}$, let $\Gamma=\{1,2,\ldots,K\}$ is a countable label set, where $l_i\in\Gamma$ is the label associated with the pixel i. To characterize the prior knowledge of l, we assume that l is homogenous and isotropic MRF in the interior of the region while it is inhomogeneous and anisotropic MRF on the boundary, which is different from the previous MRF model[1,2,4,8]. Using the equivalence between MRF and the Gibbs distribution, the joint probability of l has the following form:

$$P(l)=\frac{1}{Z}\mathrm{e}^{-U(l)}\,, \tag{3}$$

where $Z=\int_{l\in\Gamma^N}\mathrm{e}^{-U(l)}\mathrm{d}l$ is the partition function and N is the pixel number of the image. On the 8-neighbourhood system, the pair-site cliques have four types, denoting as $c^{(1)},\ldots,c^{(4)}$. Accordingly we define the four direction neighbor system as: $N^{(t)}_i=\{j\mid(i,j)\in c^{(t)}\}$, $(t=1,\ldots,4)$. Then we can define the energy function as:

$$U(l)=\sum_{i\in S}\left[\sum_{t=1}^{4}\sum_{(i,j)\in c^{(t)}}\beta_i^{(t)}\cdot I(l_i,l_j)\right] \tag{4}$$

$$I(l_i,l_j)=\begin{cases}-1 & \text{if } l_i=l_j\\ 0 & \text{else}\end{cases}, \tag{5}$$

Where $\beta_i^{(t)}(t=1,...,4)$ is the Markov parameter describing the constraint at the point *i*. If *i* is the interior point of the region, $\beta_i^{(1)}=\beta_i^{(2)}=\beta_i^{(3)}=\beta_i^{(4)}$; while on the boundary, the four kinds of $\beta_i^{(t)}$ at pixel *i* are not always the same.

2 Method

Based on (1)~(5), the parameters are estimated via MAP rule. Let $\beta=(\beta^{(1)},\beta^{(2)},\beta^{(3)},\beta^{(4)})$, $\theta=(\mu,\sigma^2,c)$, where μ,σ^2,c are *K*-dimentional vectors. Then we should estimate the following parameter vector $\{l,\beta,\theta\}$. Suppose that the prior knowledge of θ,β is uniform, using Bayes law, we get

$$P(l,\theta,\beta\mid X)\propto P(l\mid X,\theta,\beta)\cdot P(X\mid\theta,\beta)\cdot P(\theta)\cdot P(\beta)\propto P(l\mid X,\beta)\cdot P(X\mid\theta). \tag{6}$$

The estimation for the parameters is defined as

$$(\hat{l},\hat{\theta},\hat{\beta})=\arg\max\{P(l\mid X,\beta)\cdot P(X\mid\theta)\}. \tag{7}$$

If the two product items $P(l\mid X,\beta)$ and $P(X\mid\theta)$ are maximized respectively, then (7) is maximized. So

$$\hat{\theta}=\arg\max(P(X\mid\theta)), \tag{8}$$

$$\hat{\beta}=\arg\max(P(l\mid X,\beta)), \tag{9}$$

$$\hat{l}=\arg\max(P(l\mid X,\hat{\beta})). \tag{10}$$

The estimation should be updated iteratively until convergence.

To solve (8)~(10), θ is estimated using histogram based DAEM algorithm. β is estimated using an approximate method. The update of *l* is by ICM algorithm. The details are discussed as follows.

1.3 The histogram based DAEM algorithm for estimation of θ

One general method to solve (8) is the EM algorithm, but it could only find the local optima. To improve the performance, we use a deterministic annealing EM (DAEM) algorithm for estimation, where a temperature parameter is introduced to control the annealing process and thereby the global optima could be tracked during the gradually cooling process.

We introduce a hidden variant *Y* firstly. Let $Y=[y_{pk}]$ (p=1,2,…,L; k=1,2,…,K), where y_{pk} denotes the probability of the gray level *p* belonging to the *k*-th class, *L* is the number of gray levels. Then maximization of (8) could be rewritten as $\hat{\theta}=\arg\max(\log P(X\mid\theta))$. Let

$$L(X\mid\theta)\triangleq\log(P(X\mid\theta))=\log\int P(X,Y\mid\theta)\cdot\mathrm{d}Y=\log\int\frac{P(X,Y\mid\theta)}{G(Y)}\cdot G(Y)\mathrm{d}Y\geq\int G(Y)\cdot\log P(X,Y\mid\theta)\cdot\mathrm{d}Y-\int G(Y)\cdot\log G(Y)\cdot\mathrm{d}Y\triangleq J(G(Y),\theta),$$

where $G(Y)$ is a distribution of *Y*. According to variational method: $\delta J=\langle\nabla_G J,\delta G\rangle=0$ regardless of δG, we

could derive that $G(Y)=P(X,Y|\theta)\Big/\int P(X,Y|\theta)\mathrm{d}Y$. In DAEM algorithm, a temperature parameter τ is introduced, then we could get[9]: $G_\tau(Y)=[P(X,Y|\theta)]^\tau\Big/\int[P(X,Y|\theta)]^\tau\mathrm{d}Y$. If $\tau\to 0$, the distribution of $G_\tau(Y)$ is uniform. When τ increases, $G_\tau(Y)$ changes from uniform to its posterior distribution; when $\tau=1$, $G_\tau(Y)$ become the original posterior distribution $G(Y)$ as in EM[10]. During this cooling process, we could track the global optima. Then the DAEM algorithm is expressed as:

In E-step, the expectation is

$$Q(\theta|\theta^{(t)})=E_G\{\log P(X,Y|\theta)|X,\theta^{(t)}\}=\int[\log P(X,Y|\theta)]\frac{[P(X,Y|\theta^{(t)})]^\tau}{\int[P(X,Y|\theta^{(t)})]^\tau\mathrm{d}Y}\mathrm{d}Y.$$

In M-step , the maximization is $\theta^{(t+1)}=\arg\max_\theta Q(\theta|\theta^{(t)})$. The DAEM based histogram algorithm is derived as follows:

1) $t=0$, set $\tau^{(0)}=\tau_{\min}$ $(0<\tau<1)$ and $\theta^{(0)}$;

2) Iterate the following EM step until convergence:

E-step: $$Y_{pk}^{(n)}=[c_k^{(n)}\cdot g(u_p|\mu_k^{(n)},\sigma_k^{2(n)})]^\tau\Big/\sum_{k=1}^{K}[c_k^{(n)}\cdot g(u_p|\mu_k^{(n)},\sigma_k^{2(n)})]^\tau.$$

M-step: $$c_k^{(n+1)}=\sum_{p=1}^{L}Y_{pk}^{(n)}\cdot h_X(u_p)/N,$$

$$\mu_k^{(n+1)}=\sum_{p=1}^{L}Y_{pk}^{(n)}\cdot h_X(u_p)\cdot u_p\Big/\sum_{p=1}^{L}Y_{pk}^{(n)}\cdot h_X(u_p), \tag{11}$$

$$\sigma_k^{2(n+1)}=\sum_{p=1}^{L}Y_{pk}^{(n)}\cdot h_X(u_p)\cdot[u_p-\mu_k^{(n+1)}]^2\Big/\sum_{p=1}^{L}Y_{pk}^{(n)}\cdot h_X(u_p).$$

3) let t=t+1, increasing $\tau:\tau^{(t+1)}=\tau^{(t)}+c1*\exp(-c2*\Delta E)$

4) If $(\tau=1$ and $\|\nabla\theta\|^2<\varepsilon)$ stop, else go 2))

where $h_X(u_P)=\sum_{i\in S}count(x_i,u_p)$, $(p=1,2,\ldots,L)$, $count(a,b)=\begin{cases}1 & \text{if } a=b\\ 0 & \text{else}\end{cases}$, u_p is the gray value of the p-th level. $\tau^{(0)}$ should ensure $Q(\theta|\theta^{(0)})$ is a convex function and $\tau^{(0)}\approx 0.1$ may be enough; $\theta^{(0)}$ could be set by random initialization or clustering method. c_1, c_2 are constants which control the annealing schedule.

1.4 Using an approximate method to estimate β

The accurate estimation of β should always use sampling techniques, but it is very complex and time consuming. For simplicity, we propose an approximate method to estimate β. We know that on the boundary $\beta_i^{(t)}$ describes the direction effect at pixel i, considering the l_i inclines to attribute to the class of which the pixel gray value of $N_i^{(t)}$ are closer to that of pixel i. So we express $\beta_i^{(t)}$ by

$$\beta_i^{(t)} = \alpha \Big/ (comp(x_i, \bar{x}_j^{(t)}) + \eta) \,. \tag{12}$$

$$comp(x_i, \bar{x}_j^{(t)}) = \begin{cases} 0, & \text{if all the } l_j (j \in N_i^{(t)}, t = 1,...,4) \text{ are the same} \\ (\dfrac{x_i - \bar{x}_j^{(t)}}{\bar{\sigma}_j^{(t)}})^2, & \text{else} \end{cases},$$

$$\bar{x}_j^{(t)} = \frac{1}{2} \sum_{j \in N_i^{(t)}} x_j \,, \quad \bar{\sigma}_j^{(t)} = \frac{1}{2} \sum_{j \in N_i^{(t)}} \sigma_{l_j}$$

where α, η are const. Note that α is the factor which control the effect of MRF prior knowledge in the posterior energy.

1.5 Updating *l* using ICM

Solving (10), we should derive the posterior energy of $U(l \mid X)$ firstly. According to Gibbs distribution and Bayes law:

$$\begin{aligned} P(X \mid l) &= \mathrm{e}^{-U(X|l)} \big/ Z_1 \propto \mathrm{e}^{-U(X|l)}, \\ P(l \mid X) &= \mathrm{e}^{-U(l|X)} \big/ Z_2 \propto \mathrm{e}^{-U(l|X)}, \end{aligned} \tag{13}$$

$$P(l \mid X) = P(X \mid l) \cdot P(l) \big/ p(X) \propto P(X \mid l) \cdot P(l) \,. \tag{14}$$

substitute (3), (13) into (14) , we could derive that

$$U(l \mid X) = U(X \mid l) + U(l) + const = -\ln P(X \mid l) + U(l) + const - \ln Z_1 \,. \tag{15}$$

Note that Z_1 is a normalized constant and those constant values could be ignored in the minimization of (15). so we let

$$U(l \mid X) = U(X \mid l) + U(l) \,, \tag{16}$$

from formula (1) , we can derive that

$$P(X \mid l) = \prod_{i \in S} \prod_{k=1}^{K} [P(x_i \mid \mu_k, \sigma_k^2)]^{q(l_i,k)} \,, \tag{17}$$

where $q(l_i, k) = \begin{cases} 1 & \text{if } \ l_i = k \\ 0 & \text{else} \end{cases}$. Moreover, $U(l \mid X) = \sum_{i=1}^{N} U(l_i \mid l_{N_i}, X)$. Therefore,

$$U(l_i \mid l_{N_i}, X) = \sum_{k=1}^{K} [\frac{1}{2} \ln(\sigma_k^2) + \frac{(x_i - \mu_k)^2}{2\sigma_k^2}] \cdot q(l_i, k) + \sum_{t=1}^{4} \sum_{j \in N_i^{(t)}} \beta_i^{(t)} \cdot I(l_i, l_j) \,. \tag{18}$$

Maximize $P(l \mid X)\, P(l \mid X)$ is equivalent to minimize (16). We adopt iterated conditional modes (ICM) algorithm to update l_i sequentially via minimize (18)[11]. It yields：

$$\hat{l}_i^{(n+1)} = \arg\min \{U(l_i \mid l_{N_i}^{(n)}, X)\} \,. \tag{19}$$

The fine segmentation is implemented by interactively updating of l and β using (12), (18) and (19).

3 Experiment

The MRI used in the experiments is from a stroke patient as shown in Fig.1. Two experiments are done in this paper. (1) The comparison of DAEM algorithm and EM algorithm in estimation of SFNM parameter. (2) The comparison of the results of model 1 and model 2 in realization of fine segmentation.

Model 1: higher-lever MRF using mixture MRF we proposed.

Model 2: higher-lever MRF using inhomogeneous MRF described in Ref.[1].

In experiment (1), $\theta^{(0)}$ is set by random initialization and $\tau^{(0)}=0.59$, $c_1=0.03$, $c_2=0.1$ in DAEM. The information theoretic criteria AIC can be used to evaluate the optimal solution via minimize $AIC(K)$:

$$AIC(K)=-2\log(P(X\mid l,\hat{\theta}_{ML}))+2K, \tag{20}$$

where $\hat{\theta}_{ML}$ is the parameter estimated using DAEM or EM algorithm, $P(X\mid l,\hat{\theta}_{ML})$ is the likelihood function. K is the optimal class number in segmentation. The AIC curves from EM and DAEM algorithm are shown in Fig.2, from which we can observe two facts:

(1) The DAEM algorithm could obtain bigger and more stable likelihood values than that of EM algorithm. So, DAEM is better than EM in the sense of ML estimation.

(2) The optimal class number K is that who minimizes $AIC(K)$. From Fig.2, we could get the optimal class number in segmentation is $K=8$.

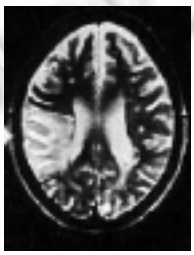

Fig.1 The original MRI of stroke

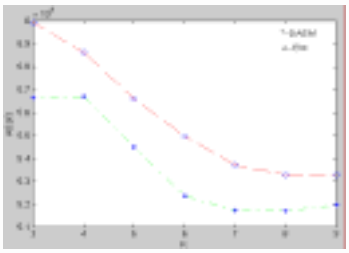

Fig.2 AIC plot from DAEM and EM algorithm

The initial segmentation using EM and DAEM are shown in Figs.3 and 4 respectively. Comparing with Fig.3, the boundary and the focus area on the left ventricle is strengthened in Fig.4. We can see clearly that using DAEM is more robust than that of using EM.

In experiment (2), we set $\alpha=0.1$, $\eta=0.5$. Figures 5 and 6 are the fine segmentation using our model and model described in Ref.[1] respectively. From the segmented image, we can see that our model has advantages of less misclassification and characterize the focus area more clearly.

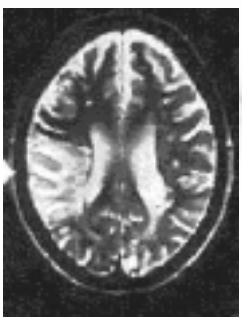

Fig.3

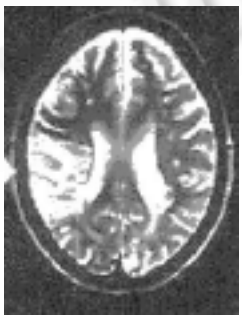

Fig.4

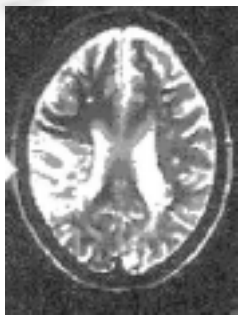

Fig.5

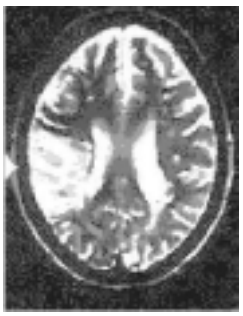

Fig.6

We use the post global relative entropy (GRE) criterion to measure the quality of the segmentation with the consideration as follows: (i) it is an objective criterion and independent of the manual segmentation reference. (ii) Based on our model, the pixel image is modeled by the SFNM, so if a segmentation method is better, its post SFNM

distribution $f_l(x)$ should be closer to its real SFNM than other method. Since the DAEM finds the unbiased estimation $f_Y(x)$ to the image histogram and we could believe it is the real SFNM. (iii) The post-GRE value could be used to measure the deviation degree between two probability distributions $f_Y(x)$ and $f_l(x)$.

Let $f_Y(x)$ denote the ML estimation of SFNM using DAEM, the parameters of $f_Y(x)$ are $\hat{\theta}_{ML}=(\hat{\mu},\hat{\sigma}^2,\hat{c})$. After fine segmentation using ICM, the SFNM parameters are estimated again using sample average method, let $f_l(x)$ denote the post segmentation SFNM, whose parameters are $\theta=(\mu,\sigma^2,c)$. Then the post-GRE value is defined by: $D(f_Y \| f_l)=\sum_{x\in\chi} f_Y(x)\cdot\log\frac{f_Y(x)}{f_l(x)}$, where x is the set of gray values.

The post-GRE segmentation criterion states that the relative entropy between the ML estimate of the SFNM and the SFNM obtained from the fine segmented image is minimal if the image components are correctly segmented. The parameter values of a particular tissue type in the estimated histogram are most likely to be equal to the parameter values of the corresponding tissue type in the fine segmented region if the pixel images are properly classified. This correspondence is lost in the case of misclassification[1,12].

So, the smaller the $D(f_l \| f_Y)$ value is, the better the segmentation will be. The closer are the two groups of parameters in Table I, the better the segmentation is. The parameters of f_Y and f_l in our approach are compared in Table I which show that they are close enough. The comparison of GRE values from different models is shown in Table II, from which we can see that our model does better segmentation in the sense of less misclassification for its smaller $D(f_Y \| f_l)$ than the model in Ref.[1].

Table 1 Real and estimated parameter values for the MRI in Fig.1

k	$c/\hat{c}$	$\mu/\hat{\mu}$	$\sigma/\hat{\sigma}$
1	0.3685/0.4286	6.2400/6.5688	3.0904/3.2217
2	0.1951/0.1432	17.5285/19.8315	7.7645/4.5155
3	0.1301/0.1266	44.2206/46.5397	18.1094/12.8614
4	0.1233/0.1031	116.3619/111.8249	34.8634/22.7968
5	0.0487/0.0531	182.7046/169.8883	22.2156/9.8605
6	0.0178/0.0259	240.7434/239.4927	6.6889/6.1829
7	0.0660/0.0718	218.0995/217.9023	9.6929/6.3589
8	0.0504/0.0478	197.0524/197.1081	18.1775/ 5.9689

Table 2 GRE value from different approach

Model	$D(f_Y \| f_l)$
Model(1)	0.0088096
Model(2)	0.0098063

We should emphasis that although we have done experiments on the brain MRI, our algorithm could be applied to other MRI segmentation cases.

4 Conclusion and Future Directions

In this paper, a hierarchical MRF model is used to characterize MRI. By using a newly presented mixture MRF model as its higher-level model, orientation is incorporated into the segmentation process. For the lower-level model, the DAEM algorithm is used to find the global optima of the SFNM parameters that avoids trapping into local optimal as compared with EM algorithm. Considering the meaning of MRF prior parameter in our model, we propose an approximate method to estimate β. The performance of the segmentation is evaluated via AIC criteria and the post-global relative entropy (GRE). The experiments show that our approach is capable of segmenting the tissue more accurately and clearly, thus facilitate further clinical analysis and diagnosis.

MRI mainly provides the anatomic information. A prospective direction is to implement segmentation via the fusion

of functional and anatomic information. We will investigate this issue in our future work.

References:

[1] Wang, Y., Adali, T., Xuan, J.H., *et al*. Magnetic resonance image analysis by information theoretic criteria and stochastic site models. IEEE Transactions on Information Technology in Biomedicine, 2001,5(2):150~158.

[2] Choi, H.S., Haynor, D.R., Kim, Y. Partial volume tissue classification of multichannel magnetic resonance images —— a mixture model. IEEE Transactions on Medical Imaging, 1994,10(9):395~407.

[3] Santago, P., Gage, H.D. Quantification of MR brain images by mixture density and partial volume modeling. IEEE Transactions on Medical Imaging, 1993,12(9):566~574.

[4] Wang, Y., Adali, T., Kung, S.Y., *et al*. Quantification and segmentation of brain tissues from MR images. IEEE Transactions on Image Processing, 1998,7(8):1165~1181.

[5] Zijdenbos, A.P., Dawant, B.M., Margolin, R.A., *et al*. Morphometric analysis of white matter lesions in MR images: method and alidation. IEEE Transactions on Image Processing, 1994,13(9):716~724.

[6] Li, S.Z. Markov random field modeling in image analysis. 2th ed., New York, Berlin Heidelberg: Springer-Verlag, 2000. 58~62.

[7] Cline, H.E., Lorensen, W.E., Kikinis, R., *et al*. Three dimensional segmentation of MR images of the head using probability and connectivity. Journal of Computer-Assisted Tomography, 1990,14:1037~1045.

[8] Liang, Z., MacFall, J.R., Harrington, D.P. Parameter estimation and tissue segmentation from multispectral MR images. IEEE Transactions on Medical Imaging, 1994,13(9):441~449.

[9] Ueda, N., Nakano, R. Deterministic annealing EM algorithm. Neural Networks, 1998,11:271~282.

[10] Dempster, A.P., Laird, N.M., Rubin, D.B. Maximum-Likelihood from incomplete data via the EM algorithm. Journal of the Royal Statistical Society, 1997,B(39):1~38.

[11] Besag, J. On the statistical analysis of dirty pictures (with discussions). Journal of the Royal Statistical Society, 1986, B(48):259~302.

[12] Cover, T.M., Thomas, J.A. Elements of Information Theory. New York: Wiley, 1991. 297~304.

基于层次 MRF 的 MR 图像分割

张红梅[1], 袁泽剑[2], 蔡忠闽[3], 卞正中[1]

[1](西安交通大学 生命科学与技术学院,陕西 西安 710049);

[2](西安交通大学 人工智能与机器人研究所,陕西 西安 710049);

[3](西安交通大学 系统工程研究所,陕西 西安 710049)

摘要: 核磁共振图像(MRI)的定量分析在神经疾病的早期治疗中有很重要作用.提出了一种基于层次 Markov 随机场模型的 MRI 图像分割新方法.在高层次的标记图象中采用了混合模型,即区域的内部用各向同性均匀 MRF 来建模,边界用各向异性非均匀 MRF 来建模.所以方向性被引入到边界信息中,这样可以更准确的表达标记图象的特性;在低层次的像素图像中,不同区域中像素的灰度分布用不同的高斯纹理来描述.分割问题可以被转换成一种最大后验概率估计问题.采用基于直方图的 DAEM 算法来估计 SNFM 参数的全局最优值;并基于 MRF 先验参数的实际意义,提出一种近似的方法来简化这些参数的估计,实验显示该方法能获得更好的结果.

关键词: 层次马尔科夫随机场;有限高斯混合体;图像分割;核磁共振图像;最大后验估计

中图法分类号: TP391 文献标识码: A